


Article

Consolidation and Dehydration Effects of Mildly Degraded Wood from Luoyang Canal No. 1 Ancient Ship

Weiwei Yang^{1,2,3}, Wanrong Ma^{1,2,3}, Xinyou Liu^{1,2,3}  and Wei Wang^{1,2,3,*}

¹ Co-Innovation Center of Efficient Processing and Utilization of Forest Resources, Nanjing Forestry University, Nanjing 210037, China; yww2000922@njfu.edu.cn (W.Y.); mawan@njfu.edu.cn (W.M.); liu.xinyou@njfu.edu.cn (X.L.)

² College of Furnishing and Industrial Design, Nanjing Forestry University, Str. Longpan No.159, Nanjing 210037, China

³ Advanced Analysis and Testing Center, Nanjing Forestry University, Str. Longpan No.159, Nanjing 210037, China

* Correspondence: wangwei1219@njfu.edu.cn; Tel.: +86-25-8542-7408

Abstract: To ensure the conservation of waterlogged archaeological wood, sustainable, safe, and effective methods must be implemented, with consolidation and dehydration being crucial for long-term preservation to maintain dimensional stability and structural integrity. This study compares the permeability of 45% methyltrimethoxysilane (MTMS) and 45% trehalose solutions to evaluate the dimensional changes, hygroscopicity, and mechanical properties of treated wood. Since the collected samples (from an ancient ship, Luoyang Canal No. 1) were mildly degraded, the drying method had a slight impact on the properties of archaeological wood. Consolidated with trehalose and MTMS agents, the longitudinal compressive strength of the waterlogged wood's cell walls increased by 66.8% and 23.5%, respectively. Trehalose proved to be more advantageous in filling pores and reducing overall shrinkage, while MTMS significantly reduced the hygroscopicity and surface hydrophilicity of the wood substance. Overall, the MTMS treatment has a smaller effect on the appearance of samples, making it more suitable for the consolidation of mildly degraded waterlogged archaeological wood.



Citation: Yang, W.; Ma, W.; Liu, X.; Wang, W. Consolidation and Dehydration Effects of Mildly Degraded Wood from Luoyang Canal No. 1 Ancient Ship. *Forests* **2024**, *15*, 1089. <https://doi.org/10.3390/f15071089>

Academic Editor: Jesús Julio Camarero

Received: 5 June 2024

Revised: 15 June 2024

Accepted: 21 June 2024

Published: 23 June 2024



Copyright: © 2024 by the authors. Licensee MDPI, Basel, Switzerland. This article is an open access article distributed under the terms and conditions of the Creative Commons Attribution (CC BY) license (<https://creativecommons.org/licenses/by/4.0/>).

Keywords: waterlogged archaeological wood; mechanical properties; chemical properties; dimensional stability; methyltrimethoxysilane; trehalose; morphological characteristics

1. Introduction

As a renewable natural polymer, wood has been extensively used in numerous human activities throughout history owing to its superior properties, abundant availability, and ease of processing. A significant portion of archaeological wood was waterlogged or wet when excavated [1,2]. Microbial degradation weakens cell walls by decomposing cellulose and hemicellulose polymers [3–5]. Although this deterioration may not be visually apparent, wood becomes highly susceptible to irreversible shrinkage and cracking upon drying [6,7]. Consequently, consolidants that reinforce cell walls and prevent collapse by filling pores and micropores are essential for long-term preservation.

Early attempts to conserve waterlogged wood involved the use of oils, waxes, and alum ($KAl(SO_4)_2 \cdot 12H_2O$), but these failed to provide adequate reinforcement [8,9]. Currently, polyethylene glycol (PEG) is the most common consolidant, and it has been widely used in the cases of the Vasa warship [10–12], Mary Rose [13], Bremen Cog [14], and other waterlogged wooden artifacts due to its non-toxicity, cost-effectiveness, and ability to enhance dimensional stability. However, PEG-treated wood is more sensitive to heat, metal ions, salts, and microbial degradation [9,15]. The decomposition products of PEG, such as formic acid, can further chemically degrade the wood, posing a threat to its long-term preservation [16].

The conservation of waterlogged archaeological wood (WAW) necessitates a safe and sustainable approach, with the consolidation process being reversible and free from inducing subsequent degradation [17]. Non-reducing sugars, such as trehalose, have shown promise as consolidants for WAW due to their stability and antioxidant capabilities [18–21] and can markedly enhance the dimensional stability and bending performance of waterlogged archaeological wood. Trehalose, with its low molecular mass, offers advantages over PEG in terms of its ability to improve mechanical properties and its conservation effectiveness [22]. Therefore, investigating the application of trehalose as a consolidant for WAW may offer a promising alternative to conventional PEG treatments.

It has been proven by many researchers that by using organosilicons, according to the type of functional group within the silane molecule, the consequent chemical modification of waterlogged wood can enhance decay resistance as well as dimensional stability [23–25]. A study by Broada et al. [26] revealed that methyltrimethoxysilane (MTMS) can effectively encrust and cover the microstructure of WAW. Recent studies have confirmed that MTMS is also satisfactory in reducing the hygroscopicity of treated wood [27,28]. Since MTMS molecules are able to penetrate and form a uniform coating on the cell wall surface, the pore area of WAW can be filled effectively.

The dehydration process also plays a crucial role in stabilizing the wood and reducing the risk of shrinkage and microbial degradation post-excavation [29]. Compared to sound wood, multiple deterioration factors weaken the structure of WAW, making the cell walls more susceptible to collapse due to capillary forces and the high surface tension of evaporating water [30]. Specialized drying should therefore take place under strictly controlled conditions. Vacuum freeze-drying and long-lasting air-drying are the most common approaches for waterlogged archaeological wood dehydration [31]. The application of these methods varies depending on the anatomical characteristics of the wood, the degree of degradation, and the size of the object to be treated. For instance, slow air-drying requires careful monitoring of the temperature and humidity to ensure gradual and uniform dehydration without causing damage to the wood. Vacuum freeze-drying is particularly suitable for delicate or highly degraded wood that may be prone to collapse during traditional drying methods [18]. This approach proved to be effective in removing moisture from wood while minimizing the risks of structural destruction, shrinkage, and cracking, but it is less applicable for large pieces [32]. Moreover, supercritical CO₂ fluid dehydration as a method of preservation has also been investigated, which utilizes CO₂'s excellent solubility and heat transfer properties to dissolve moisture from WAW.

The purpose of this research was to determine the influences of trehalose and MTMS consolidation on the mechanical properties, dimensional stability, and hygroscopicity of WAW. *Ulmus* samples from the mildly degraded ancient ship of Luoyang Canal No. 1 were employed [33] using various drying methods. Statistical analyses were also involved in evaluating the effectiveness of both the consolidation and dehydration processes. The findings presented in this paper will serve as important references for future generations, enabling such historical treasures to be properly preserved.

2. Materials and Methods

2.1. Materials

Waterlogged elm (*Ulmus parvifolia* Jacq.) wrecks from the Luoyang Canal No. 1 ancient ship (Figure 1a) [33] were cut into 90 pieces measuring 30 × 30 × 10 mm (longitudinal direction × tangential direction × radial direction) for experiments. The objects were classified as mildly degraded with an average maximum moisture content of 212.03 ± 28.33% and a basic density of 0.396 ± 0.015 g/cm³ [34].



Figure 1. Samples from the ancient ship “Luoyang Canal No. 1” (a) the excavated ship planks and (b) samples submerged in consolidants. Note: The Chinese word “海藻糖” in the (b) means trehalose.

Methyltrimethoxysilane (MTMS) and trehalose were used as consolidation agents for waterlogged wood treatment, which were provided by Macklin Ltd., Shanghai, China.

2.2. Methods

2.2.1. Consolidation Process

The specimens were initially immersed in a 70% ethanol solution for one week and subsequently transferred to a 96% ethanol solution for another week. This process led to a decrease in the moisture content ranging from 78% to 109%, as indicated by the alteration in the ethanol concentration. Subsequently, the samples were randomly divided into three groups: the first group remained untreated as a control group, the second was submerged in a 45% solution of D-trehalose consolidation for 14 days, and the third group was immersed in a 45% solution of MTMS for the same period of time (Figure 1b).

2.2.2. Dehydration and Air Conditioning

Each group of the aforementioned samples were dehydrated under the low-temperature; high-humidity (LT-HH); vacuum-freezing (VF), and supercritical CO₂(SC) drying methods, respectively. In LT-HH air-drying, the specimens were conditioned at 45 °C with 70% relative humidity until they were absolutely dry (the mass difference between two consecutive measurements was less than 0.2%). Vacuum freeze-drying and supercritical CO₂ fluid dehydration processes were carried out following the methods established in previous studies [35–37].

To examine the hygroscopicity of treated/untreated wood, all specimens were re-conditioned at 20 °C and 65%, from which the hygroscopic equilibrium moisture content was determined.

2.2.3. Mechanical Properties and Morphological Characteristics

The destructive loading test was performed with a Shimadzu universal testing instrument, AGS-X (Shimadzu Corporation, Kyoto, Japan), following ISO 13061-17 (2017) [38]. The specimens were placed at the center of the spherical movable support of the testing machine, loaded at a uniform speed, and broken within 1.0 to 5.0 min. The mean forces of 5 samples were recorded, and compressive strength was calculated using the following equation:

$$\sigma_0 = \frac{P_{\max}}{bt} \quad (1)$$

where σ_0 represents the longitudinal compressive strength of dried specimens (MPa), P_{\max} is the maximum destructive load (N), and b and t represent the width and thickness of the wood specimens (mm), respectively.

To observe the morphology of wood cells, specimens were imaged in the Hitachi S-3400N II Scanning Electron Microscope (SEM) (Hitachi Ltd., Tokyo, Japan).

2.2.4. Dimensional Stability

Physical parameters, including the shrinkage/swelling rate and weight percent gain (WPG), were measured. The effectiveness of the consolidation treatment was calculated as the weight percent gain (WPG), which was determined by the differences in the dry weight of the sample before (W_0) and after impregnation (W_1), using the following formula [39]:

$$\text{WPG} = \frac{W_0 - W_1}{W_0} \times 100\% \quad (2)$$

Linear wood shrinkage/swelling in tangential, radial, and longitudinal directions was calculated using the following equation [16]:

$$\beta = \frac{l_0 - l_1}{l_0} \times 100\% \quad (3)$$

where β represents the linear wood shrinkage/swelling (%), and l_0 and l_1 represent the initial and final lengths of waterlogged/dried wood samples (cm), respectively.

The volumetric shrinkage/swelling rate can be calculated as follows [40]:

$$\gamma = \frac{V_0 - V_1}{V_0} \times 100\% \quad (4)$$

where γ is the volumetric shrinkage/swelling (%), and V_0 and V_1 are the initial and final volumes of waterlogged/dried wood samples (cm^3), respectively.

The results of these physical characteristics were then examined by SAS (version 9.4, SAS Institute, Cary, NC, USA) to investigate their statistical significance.

2.2.5. Surface Hydrophilicity

The hydrophilicity of WAW specimens before and after the treatments was evaluated using a Drop Shape Analyzer (Model: DSA100S, Kruss, Germany). Distilled water droplets were used to record the state of the water droplet on the tangential section of the dehydrated wood surfaces, and the contact angle (θ) was then calculated through a water droplet image analysis.

2.2.6. Chemical Properties Analysis Using FT-IR

To investigate the chemical changes in WAW after reinforcement, samples from the control group and the consolidated group were ground, sieved through an 80-mesh sieve, and prepared as KBr pellets. The prepared samples were subjected to FT-IR analysis using a standard FTIR spectrometer (Tensor 27, Bruker, Germany), with 32 scans conducted at a resolution of 4 cm^{-1} over the 700 to 4000 cm^{-1} wavenumber range.

3. Results and Discussion

3.1. Mechanical Properties and Morphological Characteristics

The compressive strength (MPa) results of different wood samples vary significantly among the groups (Figure 2). The untreated archaeological wood (control) exhibited a compressive strength of 41.70 MPa, while the recent sound wood displayed a higher strength of 60.46 MPa. The wood treated with trehalose (Tre) demonstrated the highest compressive strength at 69.54 MPa, indicating a significant enhancement in strength due to the trehalose treatment. In contrast, the wood treated with Trimethoxymethylsilane (MTMS) showed a

lower compressive strength of 51.49 MPa compared to the trehalose-treated and healthy wood samples [41].

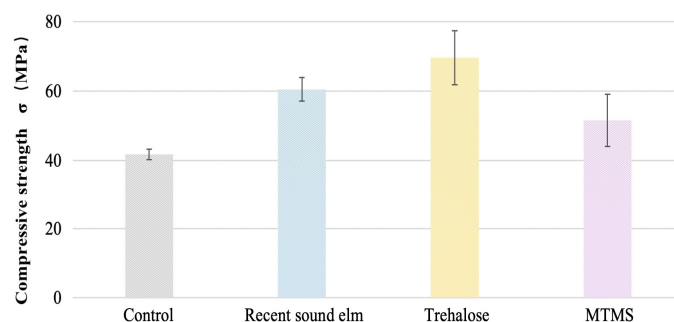


Figure 2. Compressive strength (MPa) of recent sound elm, untreated archaeological wood (control), and samples treated with trehalose and MTMS.

Figure 3 illustrates the visual effects of the MTMS and trehalose treatments on the waterlogged wood samples compared to the untreated samples. The MTMS-treated wood shows a noticeable change in color, with the treated samples appearing significantly darker and more uniform than the untreated ones. This suggests that MTMS treatment impacts the surface coloration, likely due to the formation of a siloxane network within the wood structure. In contrast, the trehalose-treated wood exhibits a lighter and more even coloration, indicating that trehalose treatment does not significantly darken the wood's surface, possibly due to its different interaction with the wood structure, forming hydrogen bonds rather than a siloxane network. Both treatments result in a more uniform surface texture compared to the untreated samples, implying improved structural consolidation. These visual differences underscore that while both MTMS and trehalose effectively consolidate and stabilize waterlogged wood, they do so in ways that differently impact the wood's surface appearance and internal structure, aligning with previous findings about their unique advantages in preserving archaeological wood.

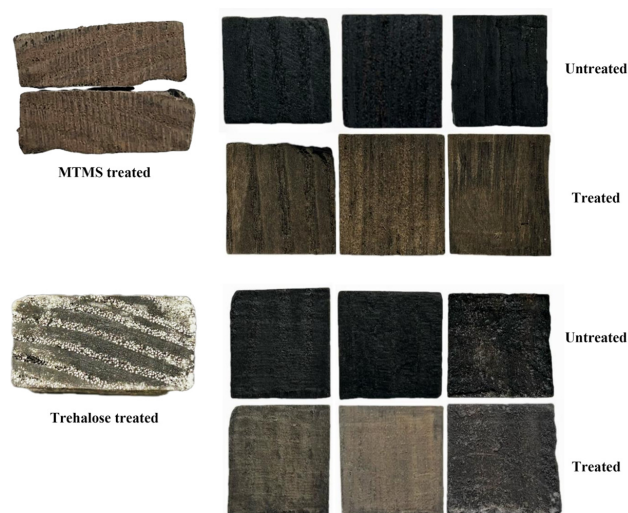


Figure 3. Cross-section and radial-section photographs of wood samples after MTMS and trehalose reinforcement.

A SEM analysis of the treated and untreated samples (Figure 4) confirmed these mechanical properties. Both the MTMS and trehalose solvents effectively penetrated the cell walls to form a thick coating on their surfaces and filled the cell lumina. Comparative observations of SEM images in the tangential section revealed that trehalose deposition filled the cell wall pits more efficiently than MTMS.

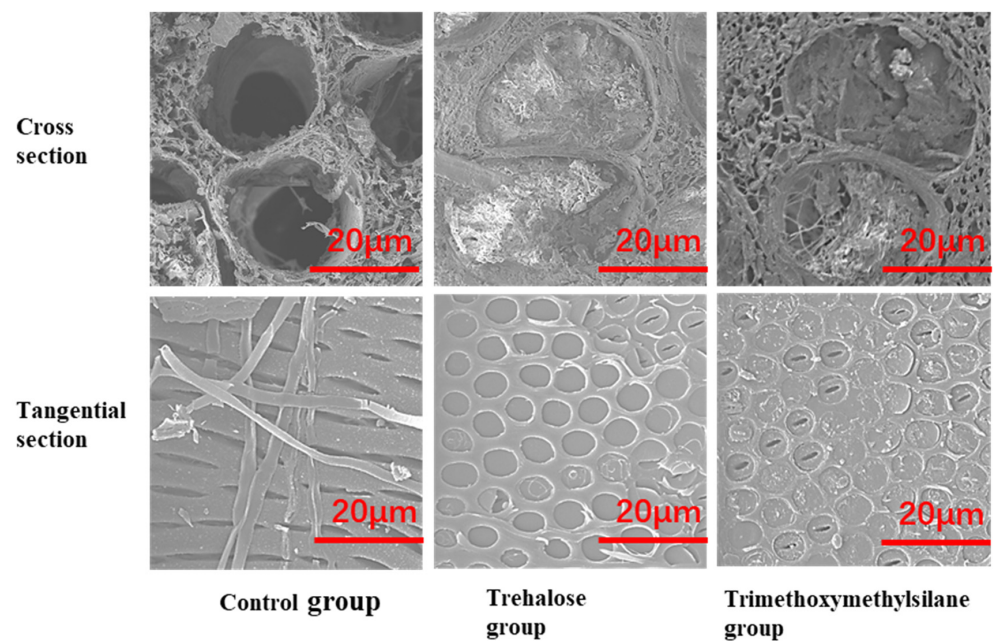


Figure 4. Scanning electron microscope (SEM) images of archaeological wood samples in the cross section and tangential section.

3.2. Evaluation of Dimensional Stability

The results of the weight percent gain (WPG) and shrinkage rate of the untreated and consolidated archaeological elm dried under various conditions are presented in Tables 1 and 2.

Table 1. Average weight percent gain (WPG) and shrinkage of waterlogged archaeological wood samples unmodified and modified with trehalose and MTMS, respectively.

Consolidation Treatment	WPG (%)	Shrinkage (%)			
		Tangential	Radial	Longitudinal	Volume
Control (untreated)	-	6.61	5.18	1.46	13.8
Trehalose	92.19	2.49	1.88	0.97	5.46
MTMS	44.63	3.65	3.82	0.68	8.33
<i>p</i> -value	<0.001	<0.001	<0.001	0.012	<0.001

Table 2. Average weight percent gain (WPG) and shrinkage of waterlogged archaeological wood samples that were low-temperature, high-humidity dried (LT-HH-D), vacuum freeze-dried (VF-D), and supercritical CO₂ fluid-dried (SC-D), respectively.

Dehydration Method	WPG (%)	Shrinkage (%)			
		Tangential	Radial	Longitudinal	Volume
LT-HH-D	80.97	3.08	3.22	0.72	7.24
VF-D	69.48	4.14	4.04	0.66	9.06
SC-D	54.78	3.52	2.30	1.36	7.34
<i>p</i> -value	0.042	0.496	0.005	0.004	0.088

It is evident that the retention of both consolidants corresponds to wood shrinkage and weight change regardless of the drying method employed. This observation agrees with the SEM images, which show that the vessels and wood fiber cells were sufficiently filled. Compared with the untreated wood, the trehalose and MTMS interventions reduced the shrinkage rate by approximately 50% or greater either in the three

anatomical directions or in the total volume of specimens. Similar results were observed by Broda et al. and Kennedy et al. [42–47], where physical measurements revealed that the decreased porosity may contribute to less shrinkage and swelling in archaeological wood [27].

The reduced porosity in waterlogged wood helps preserve the structural integrity of the wood cell walls, which, in turn, reduces volume loss and directly minimizes overall dimensional changes [48–50]. This effect was particularly evident in the case of the trehalose-treated samples (Table 1), where the agent most substantially limited wood shrinkage and caused the highest WPG.

The relatively higher density of trehalose (378.3 g/mol) may contribute to the WPG value being twice as much as that observed with the MTMS treatment (136.22 g/mol). Different chemical interactions between the two consolidants and the wood also have an impact. Trehalose can form hydrogen bonds with the hydroxyl groups in the cellulose of the wood, leading to more effective penetration into the wood material. MTMS, on the other hand, primarily forms a siloxane network on the surface, which might not contribute as significantly to weight gain [42,43]. For comparison, with severely degraded wood, the WPG values could reach approximately 200% after consolidation [46–52], whereas this rate is obviously lower in Table 1, primarily because the specimens used were only mildly degraded [33].

Moreover, *p*-values less than 0.001 based on the SAS analysis indicate that the consolidation process has a significant effect on the WPG and shrinkage rate. It is noticeable that the drying conditions do not present strong relevance with the dimensional stability of the archaeological wood samples in this study.

3.3. Hygroscopicity of Treated Wood

To estimate the effects of the treatments with respect to moisture absorption, the archeological wood samples were conditioned at 20 °C with 65%RH until reaching EMC [53,54].

Table 3 presents the hygroscopicity of the WAW samples. Due to the decay of cellulosic fraction [55,56], the most pronounced swelling was observed in the unreinforced group, where the volumetric swelling reached up to 7.21%, while 4.99% and 2.06% swelling were measured in the tangential and radial directions, respectively.

Table 3. The average swelling rate (%), absorption equilibrium moisture content (%), and surface contact angle (°) of the treated and untreated WAW specimens.

Specimens	Swelling (%)	EMC at 65%RH (%)	Contact Angle (°)
Control	Tangential	4.99	12.68 ± 0.90
	Radial	2.06	
	Longitudinal	0.30	
	Volume	7.21	
Trehalose (Tre)	Tangential	2.01	11.18 ± 0.57
	Radial	1.82	
	Longitudinal	0.31	
	Volume	4.08	
Trimethoxymethylsilane (MTMS)	Tangential	2.75	8.01 ± 0.46
	Radial	1.11	
	Longitudinal	0.28	
	Volume	4.09	

MTMS and trehalose proved to be efficient in decreasing moisture absorption. The swelling rate demonstrated in Table 3 suggests that there is no significant difference between consolidated specimens, whereas the hydrophilicity of wood is variable after air humidity conditioning. Despite the fact that the hygroscopicity of wood was permanently reduced at a higher relative humidity after the initial desorption, the trehalose-

treated samples presented an equilibrium moisture content of 11.18%, indicating that trehalose is less capable of reducing the hygroscopicity of consolidated wood. For comparison, this value presented a 4.6% decrease after MTMS reinforcement, which implies that the absorption behavior was diminished. The results are in line with the desorption and adsorption isotherms depicted with the GAB model, as Tahira et al. [21] and Majka et al. [57] reported in their previous studies.

The surface hydrophobicity of the untreated samples (control) and those treated with MTMS and trehalose is reflected by the contact angle values (Table 3). It is clearly revealed that the modification of the initial wetting behavior occurred on waterlogged elm surfaces after reinforcement. The mean water contact angle on the untreated sample surface is 36.4° , which is typical of hydrophilic wood ($<65^\circ$). The largest contact angle θ was observed in the MTMS-treated samples, suggesting that MTMS conservation improved the hydrophobicity of waterlogged archaeological wood [58,59].

3.4. Chemical Properties

To confirm the presence of disaccharides and organosilicons inside the treated wood samples, FT-IR analyses were performed, as shown in Figure 5.

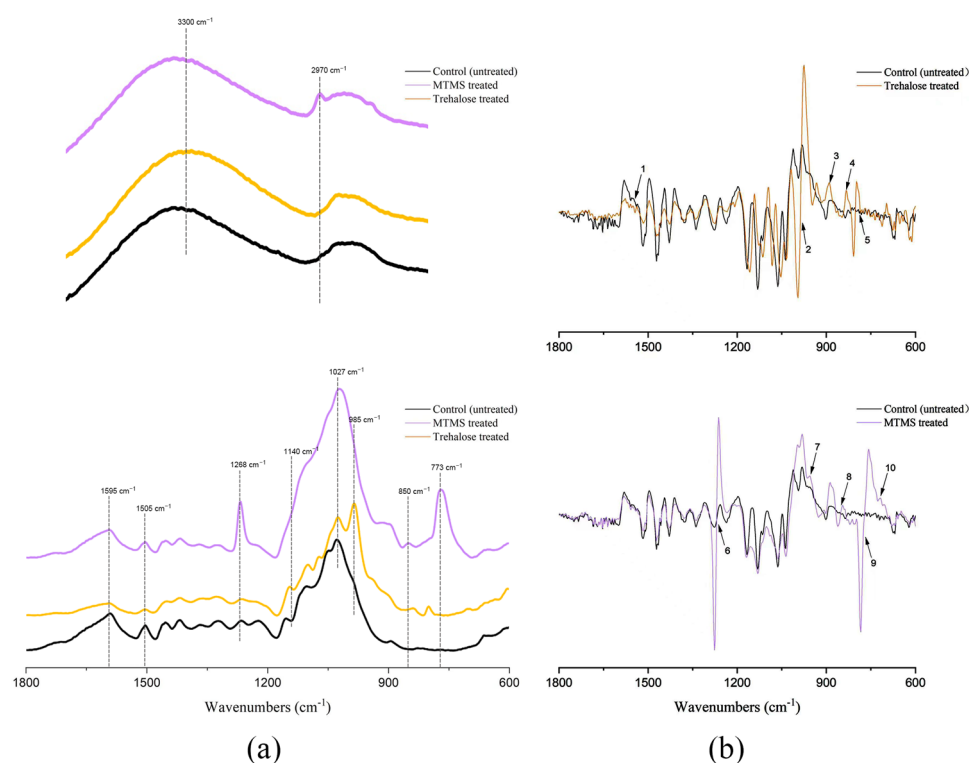


Figure 5. FT-IR spectra (a) and their derivatives (b) of untreated, trehalose-treated, and MTMS-treated WAW.

Compared to the untreated spectrum, the spectra of the samples treated with MTMS and trehalose appear to decrease in intensity during the band from 3600 to 3100 cm^{-1} , indicating that the hydroxyl groups assigned to this region are less available due to their reaction with consolidants. The reduction in the accessible hydroxyl groups was also evidenced by the aforementioned hygroscopicity experiments, revealing that the wood treatment caused reductions in the equilibrium moisture content and sorption hysteresis in comparison with the untreated wood [27,42]. The wood samples treated with MTMS show the presence of a strong absorption band at 2970 cm^{-1} assigned to the symmetric stretching vibration of the C-H bonds in CH_3 groups in wood and silanes.

Greater differences can be observed in the fingerprint region (Figure 5a). In order to identify the interactions between the consolidate solvent and the wood substrate, derivatives were plotted to record the slope variation in the FT-IR spectra (Figure 5b). The MTMS and trehalose spectra present lower intensities for the bands between 1595 and 1505 cm^{-1} (1), suggesting the alteration in C=C stretching assigned to lignin [60,61]. For the MTMS-treated spectrum, the distinguishable strong absorption at 1268 cm^{-1} (6) may be attributed to the Si-C stretching vibration in Si-CH₃. The same behaviors show bands from 1140, 1027, 850 (8), and 773 (9) cm^{-1} in the silane spectrum, which demonstrate the symmetric and asymmetric stretching vibrations of Si-C, Si-O-C, Si-O-Si, and C-O, as well as the -Si-C rocking in -SiCH₃ [62–70].

It is thought that the main difference in mechanism between organosilicons and sugar treatment lies in their modes of interaction with the wood structure [43]. Owing to the reaction with hydroxyl groups, MTMS is able to form siloxy bands (Si-O-C) and potentially create a spatial network that binds wood polymers together, which would explain the appearance of the bands near 850 (8) and 715 (10) cm^{-1} in the derivative spectrum (Figure 5b). The analyzed spectrum of the samples treated with trehalose at 890 (3) and 835 (2) cm^{-1} clearly indicate their presence in the wood. Han et al. interpreted the band at 995 cm^{-1} as a characteristic absorption of trehalose due to unique molecular vibrations involving their structural groups [71]. The feature is also shown in Figure 5b, as arrow 3 points out.

4. Discussion

The results indicate that trehalose treatment significantly enhances the compressive strength of archaeological wood, surpassing the strengths of both untreated and MTMS-treated wood. The SEM analysis supports these findings, showing that trehalose more effectively fills cell wall pits compared to MTMS, thereby contributing to the higher compressive strength. This suggests that trehalose is a more effective consolidant for improving the mechanical properties of degraded wood. The weight percent gain and shrinkage data highlight the effectiveness of trehalose and MTMS in stabilizing archaeological wood. The substantial reduction in shrinkage rates and the significant weight gains, particularly with trehalose, indicate a strong interaction between the consolidants and the wood structure. Trehalose's higher molecular weight and its ability to form hydrogen bonds with cellulose hydroxyl groups likely contribute to its superior performance in limiting shrinkage and enhancing dimensional stability compared to MTMS. The hygroscopicity results show that both the trehalose and MTMS treatments reduce moisture absorption in archaeological wood, with MTMS being slightly more effective in reducing the equilibrium moisture content. However, the trehalose-treated samples still exhibit considerable improvements in hygroscopicity and surface hydrophobicity, as evidenced by the contact angle measurements. This indicates that while MTMS might offer better moisture resistance, trehalose also significantly enhances wood's resistance to moisture absorption. The FT-IR analysis reveals that both the trehalose and MTMS treatments result in a decrease in the availability of hydroxyl groups, supporting the observed reduction in hygroscopicity. The specific absorption bands in the MTMS-treated wood spectrum suggest the formation of a siloxane network, while the trehalose-treated wood spectrum indicates the presence of trehalose molecules. These chemical interactions highlight the different mechanisms by which trehalose and MTMS consolidate and stabilize the wood structure, with trehalose forming hydrogen bonds and MTMS creating a siloxane network. Overall, the findings demonstrate that trehalose is highly effective in improving the mechanical properties, dimensional stability, and moisture resistance of archaeological wood, making it a superior consolidant compared to MTMS for the preservation of mildly-degraded waterlogged wood.

5. Conclusions

Trehalose and MTMS treatments significantly enhanced the mechanical properties of waterlogged wood cell walls, with MTMS increasing the strength by 1.23 times and trehalose increasing the strength by 1.67 times. These treatments also improved the dimensional stability of the specimens, with MTMS achieving a 39.6% improvement and trehalose achieving an even more impressive 60.4% enhancement. MTMS proved to be a versatile stabilizing agent, particularly effective in reducing the hygroscopicity of the waterlogged *Ulmus* samples. Despite causing a slightly darker surface coloration, trehalose can also be considered satisfactory in strengthening the mechanical properties and dimensional stability of archaeological wood. The FT-IR and derivative spectra analyses provided further evidence that both treatments contribute to the consolidation of the wood structure by bulking the cell walls or filling the lumina. These chemical interactions underscore the efficacy of both trehalose and MTMS in preserving and stabilizing waterlogged archaeological wood, each offering unique advantages.

Author Contributions: Conceptualization, W.Y., X.L. and W.W.; methodology, W.Y. and X.L.; software, W.Y. and W.M.; validation, W.Y., W.W. and X.L.; formal analysis, W.Y., W.M. and X.L.; investigation, W.Y., W.W. and X.L.; data curation, W.Y., W.W. and X.L.; writing—original draft preparation, W.Y., X.L. and W.W.; writing—review and editing, W.W. and X.L.; visualization, X.L.; supervision, W.W. All authors have read and agreed to the published version of the manuscript.

Funding: This work was funded by the Nanjing Forestry University Foundation for Basic Research, Grant No. 163104127, and the Priority Academic Program Development (PAPD) of Jiangsu Province, China.

Data Availability Statement: The raw data supporting the conclusions of this article will be made available by the authors upon request.

Acknowledgments: The authors would like to thank the College of Furnishings and Industrial Design, Nanjing Forestry University for providing the experimental conditions.

Conflicts of Interest: The authors declare no conflicts of interest.

References

1. Singh, A.P.; Kim, Y.S.; Chavan, R.R. Advances in Understanding Microbial Deterioration of Buried and Waterlogged Archaeological Woods: A Review. *Forests* **2022**, *13*, 394. [[CrossRef](#)]
2. Welling, J.; Schwarz, T.; Bauch, J. Biological, Chemical and Technological Characteristics of Waterlogged Archaeological Piles (*Quercus Petraea* (Matt.) Liebl.) of a Medieval Bridge Foundation in Bavaria. *Eur. J. Wood Prod.* **2018**, *76*, 1173–1186. [[CrossRef](#)]
3. Weimer, P.J. Degradation of Cellulose and Hemicellulose by Ruminant Microorganisms. *Microorganisms* **2022**, *10*, 2345. [[CrossRef](#)]
4. Reese, E.T. Degradation of Polymeric Carbohydrates by Microbial Enzymes. In *The Structure, Biosynthesis, and Degradation of Wood*; Loewus, F.A., Runeckles, V.C., Eds.; Springer: Boston, MA, USA, 1977; pp. 311–367.
5. Christensen, M.; Frosch, M.; Jensen, P.; Schnell, U.; Shashoua, Y.; Nielsen, O.F. Waterlogged Archaeological Wood—Chemical Changes by Conservation and Degradation. *J. Raman Spectrosc.* **2006**, *37*, 1171–1178. [[CrossRef](#)]
6. Walsh-Korb, Z.; Avérous, L. Recent Developments in the Conservation of Materials Properties of Historical Wood. *Prog. Mater. Sci.* **2019**, *102*, 167–221. [[CrossRef](#)]
7. Blanchette, R.A. A Review of Microbial Deterioration Found in Archaeological Wood from Different Environments. *Int. Biodeterior. Biodegrad.* **2000**, *46*, 189–204. [[CrossRef](#)]
8. Braovac, S.; McQueen, C.M.A.; Sahlstedt, M.; Kutzke, H.; Lucejko, J.J.; Klokkernes, T. Navigating Conservation Strategies: Linking Material Research on Alum-Treated Wood from the Oseberg Collection to Conservation Decisions. *Herit. Sci.* **2018**, *6*, 77. [[CrossRef](#)]
9. Zoia, L.; Tamburini, D.; Orlandi, M.; Lucejko, J.J.; Salanti, A.; Tolppa, E.-L.; Modugno, F.; Colombini, M.P. Chemical Characterisation of the Whole Plant Cell Wall of Archaeological Wood: An Integrated Approach. *Anal. Bioanal. Chem.* **2017**, *409*, 4233–4245. [[CrossRef](#)]
10. Seborg, R.M.; Inverarity, R.B. Preservation of Old, Waterlogged Wood by Treatment with Polyethylene Glycol. *Science* **1962**, *136*, 649–650. [[CrossRef](#)]

11. Hocker, E.; Almkvist, G.; Sahlstedt, M. The Vasa Experience with Polyethylene Glycol: A Conservator's Perspective. *J. Cult. Herit.* **2012**, *13*, S175–S182. [[CrossRef](#)]
12. Wagner, L.; Almkvist, G.; Bader, T.K.; Bjurhager, I.; Rautkari, L.; Gamstedt, E.K. The Influence of Chemical Degradation and Polyethylene Glycol on Moisture-Dependent Cell Wall Properties of Archeological Wooden Objects: A Case Study of the Vasa Shipwreck. *Wood Sci. Technol.* **2016**, *50*, 1103–1123. [[CrossRef](#)]
13. Fors, Y.; Sandström, M. Sulfur and Iron in Shipwrecks Cause Conservation Concerns. *Chem. Soc. Rev.* **2006**, *35*, 399–415. [[CrossRef](#)] [[PubMed](#)]
14. Hoffmann, P.; Singh, A.; Kim, Y.S.; Wi, S.G.; Kim, I.-J.; Schmitt, U. The Bremen Cog of 1380—An Electron Microscopic Study of Its Degraded Wood before and after Stabilization with PEG. *Holzforschung* **2004**, *58*, 211–218. [[CrossRef](#)]
15. Glastrup, J.; Shashoua, Y.; Egsgaard, H.; Mortensen, M.N. Degradation of PEG in the Warship Vasa. *Macromol. Symp.* **2006**, *238*, 22–29. [[CrossRef](#)]
16. Broda, M.; Mazela, B.; Radka, K. Methyltrimethoxysilane as a Stabilising Agent for Archaeological Waterlogged Wood Differing in the Degree of Degradation. *J. Cult. Herit.* **2019**, *35*, 129–139. [[CrossRef](#)]
17. Bugani, S.; Cloetens, P.; Colombini, M.; Giachi, G.; Janssens, K.; Modugno, F.; Morselli, L.; Van de Casteele, E. Evaluation of Conservation Treatments for Archaeological Waterlogged Wooden Artefacts. In Proceedings of the 9th International Conference on NDT of Art, Jerusalem, Israel, 25 May 2008; pp. 25–30.
18. Jones, S.P.; Slater, N.K.; Jones, M.; Ward, K.; Smith, A.D. Investigating the Processes Necessary for Satisfactory Freeze-Drying of Waterlogged Archaeological Wood. *J. Archaeol. Sci.* **2009**, *36*, 2177–2183. [[CrossRef](#)]
19. Giachi, G.; Capretti, C.; Macchioni, N.; Pizzo, B.; Donato, I.D. A Methodological Approach in the Evaluation of the Efficacy of Treatments for the Dimensional Stabilisation of Waterlogged Archaeological Wood. *J. Cult. Herit.* **2010**, *11*, 91–101. [[CrossRef](#)]
20. Gallina, M.E.; Sassi, P.; Paolantoni, M.; Morresi, A.; Cataliotti, R.S. Vibrational Analysis of Molecular Interactions in Aqueous Glucose Solutions. Temperature and Concentration Effects. *J. Phys. Chem. B* **2006**, *110*, 8856–8864. [[CrossRef](#)] [[PubMed](#)]
21. Tahira, A.; Howard, W.; Pennington, E.R.; Kennedy, A. Mechanical Strength Studies on Degraded Waterlogged Wood Treated with Sugars. *Stud. Conserv.* **2017**, *62*, 223–228. [[CrossRef](#)]
22. Imazu, S.; Morgos, A. Conservation of Waterlogged Wood Using Sugar Alcohol and Comparison the Effectiveness of Lactitol, Sucrose and PEG 4000 Treatment. In Proceedings of the 6th ICOM Group on Wet Organic Archaeological Materials Conference, York, UK, 9–13 September 1997; pp. 235–254.
23. Mai, C.; Militz, H. Modification of Wood with Silicon Compounds. Treatment Systems Based on Organic Silicon Compounds? A Review. *Wood Sci. Technol.* **2004**, *37*, 453–461. [[CrossRef](#)]
24. Donath, S.; Militz, H.; Mai, C. Creating Water-Repellent Effects on Wood by Treatment with Silanes. *Holzforschung* **2006**, *60*, 40–46. [[CrossRef](#)]
25. Giudice, C.A.; Alfieri, P.V.; Canosa, G. Decay Resistance and Dimensional Stability of Araucaria Angustifolia Using Siloxanes Synthesized by Sol–Gel Process. *Int. Biodeterior. Biodegrad.* **2013**, *83*, 166–170. [[CrossRef](#)]
26. Broda, M.; Mazela, B. Application of Methyltrimethoxysilane to Increase Dimensional Stability of Waterlogged Wood. *J. Cult. Herit.* **2017**, *25*, 149–156. [[CrossRef](#)]
27. Broda, M.; Curling, S.F.; Spear, M.J.; Hill, C.A.S. Effect of Methyltrimethoxysilane Impregnation on the Cell Wall Porosity and Water Vapour Sorption of Archaeological Waterlogged Oak. *Wood Sci. Technol.* **2019**, *53*, 703–726. [[CrossRef](#)]
28. Broda, M.; Plaza, N.Z. Durability of Model Degraded Wood Treated with Organosilicon Compounds against Fungal Decay. *Int. Biodeterior. Biodegrad.* **2023**, *178*, 105562. [[CrossRef](#)]
29. Nguyen, T.D.; Sakakibara, K.; Imai, T.; Tsujii, Y.; Kohdzuma, Y.; Sugiyama, J. Shrinkage and swelling behavior of archaeological waterlogged wood preserved with slightly crosslinked sodium polyacrylate. *J. Wood Sci.* **2018**, *64*, 294–300. [[CrossRef](#)]
30. Fejfer, M.; Majka, J.; Zborowska, M. Dimensional Stability of Waterlogged Scots Pine Wood Treated with PEG and Dried Using an Alternative Approach. *Forests* **2020**, *11*, 1254. [[CrossRef](#)]
31. Liu, X.; Tu, X.; Ma, W.; Zhang, C.; Huang, H.; Varodi, A.M. Consolidation and Dehydration of Waterlogged Archaeological Wood from Site Huaguangjiao No. 1. *Forests* **2022**, *13*, 1919. [[CrossRef](#)]
32. Blanchet, P.; Kaboorani, A.K.; Bustos, C. Understanding the Effects of Drying Methods on Wood Mechanical Properties at Ultra and Cellular Levels. *Wood Fiber Sci.* **2016**, *48*, 117–128.
33. Yang, W.; Ma, W.; Liu, X. Evaluation of Deterioration Degree of Archaeological Wood from Luoyang Canal No. 1 Ancient Ship. *Forests* **2024**, *15*, 963. [[CrossRef](#)]
34. Jong, J. Conservation Techniques for Old Archaeological Wood from Shipwrecks Found in The Netherlands. In *Biodeterioration Investigation Techniques*; Walters, A.H., Ed.; Applied Science: London, UK, 1977; pp. 295–338.
35. Jensen, P.; Jensen, J.B. Dynamic Model for Vacuum Freeze-Drying of Waterlogged Archaeological Wooden Artefacts. *J. Cult. Herit.* **2006**, *7*, 156–165. [[CrossRef](#)]
36. Liu, H.; Xie, J.; Zhang, J. Moisture transfer and drying stress of eucalyptus wood during supercritical CO₂ (ScCO₂) dewatering and ScCO₂ combined oven drying. *BioResources* **2022**, *17*, 5116–5128. [[CrossRef](#)]
37. Yang, L. Effect of Temperature and Pressure of Supercritical CO₂ on Dewatering, Shrinkage and Stresses of Eucalyptus Wood. *Appl. Sci.* **2021**, *11*, 8730. [[CrossRef](#)]

38. *ISO 13061-17:2017; Physical and Mechanical Properties of Wood—Test Methods for Small Clear Wood Specimens—Part 17: Determination of Ultimate Stress in Compression Parallel to Grain*. International Organization for Standardization: Geneva, Switzerland, 2017.
39. Varivodina, I.; Kosichenko, N.; Varivodin, V.; Sedliačik, J. Interconnections Among the Rate of Growth, Porosity, and Wood Water Absorption. *Wood Res.* **2010**, *55*, 59–66.
40. *ISO 13061-16:2017; Physical and Mechanical Properties of Wood—Test Methods for Small Clear Wood Specimens—Part 16: Determination of Volumetric Swelling*. International Organization for Standardization: Geneva, Switzerland, 2017.
41. Broda, M.; Spear, M.J.; Curling, S.F.; Ormondroyd, G.A. The Viscoelastic Behaviour of Waterlogged Archaeological Wood Treated with Methyltrimethoxysilane. *Materials* **2021**, *14*, 5150. [[CrossRef](#)] [[PubMed](#)]
42. Broda, M.; Majka, J.; Olek, W.; Mazela, B. Dimensional Stability and Hygroscopic Properties of Waterlogged Archaeological Wood Treated with Alkoxysilanes. *Int. Biodeterior. Biodegrad.* **2018**, *133*, 34–41. [[CrossRef](#)]
43. Broda, M.; Dąbek, I.; Dutkiewicz, A.; Dutkiewicz, M.; Popescu, C.-M.; Mazela, B.; Maciejewski, H. Organosilicons of Different Molecular Size and Chemical Structure as Consolidants for Waterlogged Archaeological Wood—A New Reversible and Retreatable Method. *Sci. Rep.* **2020**, *10*, 2188. [[CrossRef](#)] [[PubMed](#)]
44. Morgós, A.; Imazu, S.; Ito, K. Sugar Conservation of Waterlogged Archaeological Finds in the Last 30 Years. In Proceedings of the 2015 Conservation and Digitalization Conference, Gdańsk, Poland, 19–22 May 2015; pp. 15–20.
45. Kennedy, A.; Pennington, E.R. Conservation of Chemically Degraded Waterlogged Wood with Sugars. *Stud. Conserv.* **2014**, *59*, 194–201. [[CrossRef](#)]
46. Nguyen, T.D.; Kohdzuma, Y.; Endo, R.; Sugiyama, J. Evaluation of Chemical Treatments on Dimensional Stabilization of Archaeological Waterlogged Hardwoods Obtained from the Thang Long Imperial Citadel Site, Vietnam. *J. Wood Sci.* **2018**, *64*, 436–443. [[CrossRef](#)]
47. Liu, L.; Zhang, L.; Zhang, B.; Hu, Y. A Comparative Study of Reinforcement Materials for Waterlogged Wood Relics in Laboratory. *J. Cult. Herit.* **2019**, *36*, 94–102. [[CrossRef](#)]
48. Eriksson, K.-E.L.; Blanchette, R.A.; Ander, P. *Microbial and Enzymatic Degradation of Wood and Wood Components*; Springer Science & Business Media: Berlin/Heidelberg, Germany, 2012.
49. Cao, H.; Gao, X.; Chen, J.; Xi, G.; Yin, Y.; Guo, J. Changes in Moisture Characteristics of Waterlogged Archaeological Wood Owing to Microbial Degradation. *Forests* **2022**, *14*, 9. [[CrossRef](#)]
50. Babiński, L.; Fabisiak, E.; Zborowska, M.; Michalska, D.; Prądyński, W. Changes in Oak Wood Buried in Waterlogged Peat: Shrinkage as a Complementary Indicator of the Wood Degradation Rate. *Eur. J. Wood Prod.* **2019**, *77*, 691–703. [[CrossRef](#)]
51. Zhang, J.; Li, Y.; Ke, D.; Wang, C.; Pan, H.; Chen, K.; Zhang, H. Modified Lignin Nanoparticles as Potential Conservation Materials for Waterlogged Archaeological Wood. *ACS Appl. Nano Mater.* **2023**, *6*, 12351–12363. [[CrossRef](#)]
52. Endo, R.; Sugiyama, J. New Attempts with the Keratin-Metal/Magnesium Process for the Conservation of Archaeological Waterlogged Wood. *J. Cult. Herit.* **2022**, *54*, 53–58. [[CrossRef](#)]
53. Giachi, G.; Capretti, C.; Donato, I.D.; Macchioni, N.; Pizzo, B. New Trials in the Consolidation of Waterlogged Archaeological Wood with Different Acetone-Carried Products. *J. Archaeol. Sci.* **2011**, *38*, 2957–2967. [[CrossRef](#)]
54. Pecoraro, E.; Pizzo, B.; Salvini, A.; Macchioni, N. Dynamic Mechanical Analysis (DMA) at Room Temperature of Archaeological Wood Treated with Various Consolidants. *Holzforschung* **2019**, *73*, 757–772. [[CrossRef](#)]
55. Skinner, T.P.W.C. *Dimensional Stabilisation of Waterlogged Archaeological Wood: An Investigation of the Water Content of the Cell Wall of Waterlogged Archaeological Wood and Its Replacement with Water-Soluble Compounds*; University of London, University College London: London, UK, 2001.
56. Lindfors, E.-L.; Lindström, M.; Iversen, T. Polysaccharide Degradation in Waterlogged Oak Wood from the Ancient Warship Vasa. *Holzforschung* **2008**, *62*, 57–63. [[CrossRef](#)]
57. Majka, J.; Babiński, L.; Olek, W. Sorption Isotherms of Waterlogged Subfossil Scots Pine Wood Impregnated with a Lactitol and Trehalose Mixture. *Holzforschung* **2017**, *71*, 813–819. [[CrossRef](#)]
58. Zhou, Y.; Wang, K.; Hu, D. High Retreatability and Dimensional Stability of Polymer Grafted Waterlogged Archaeological Wood Achieved by ARGET ATRP. *Sci. Rep.* **2019**, *9*, 9879. [[CrossRef](#)]
59. Barkai, H.; Soumya, E.; Sadiki, M.; Mounyr, B.; Ibnsouda, K.S. Impact of Enzymatic Treatment on Wood Surface Free Energy: Contact Angle Analysis. *J. Adhes. Sci. Technol.* **2017**, *31*, 726–734. [[CrossRef](#)]
60. Broda, M.; Hill, C.A. Conservation of Waterlogged Wood—Past, Present and Future Perspectives. *Forests* **2021**, *12*, 1193. [[CrossRef](#)]
61. Colombini, M.P.; Lucejko, J.J.; Modugno, F.; Orlandi, M.; Zoia, L. A multi-analytical study of degradation of lignin in archaeological waterlogged wood. *Talanta* **2010**, *80*, 61–70. [[CrossRef](#)]
62. Popescu, M.C.; Froidevaux, J.; Navi, P.; Popescu, C.M. Structural modifications of *Tilia cordata* wood during heat treatment investigated by FT-IR and 2D IR correlation spectroscopy. *J. Mol. Struct.* **2013**, *1033*, 176–186. [[CrossRef](#)]
63. Al-Oweini, R.; El-Rassy, H. Synthesis and characterization by FTIR spectroscopy of silica aerogels prepared using several Si (OR) and R00 Si (OR)3 precursors. *J. Mol. Struct.* **2009**, *919*, 140–145. [[CrossRef](#)]
64. Benmouhoub, C.; Gauthier-Manuel, B.; Zegadi, A.; Robert, L. A Quantitative Fourier Transform Infrared Study of the Grafting of Aminosilane Layers on Lithium Niobate Surface. *Appl. Spectrosc.* **2017**, *71*, 1568–1577. [[CrossRef](#)] [[PubMed](#)]

65. Pasteur, G.A.; Schonhorn, H. Interaction of Silanes with Antimony Oxide to Facilitate Particulate Dispersion in Organic Media and to Enhance Flame Retardance. *Appl. Spectrosc.* **1975**, *29*, 512–517. [[CrossRef](#)]
66. Kavale, M.S.; Mahadik, D.B.; Parale, V.G.; Wagh, P.B.; Gupta, S.C.; Rao, A.V.; Barshilia, H.C. Optically transparent, super hydrophobic methyltrimethoxysilane based silica coatings without silylating reagent. *Appl. Surf. Sci.* **2011**, *258*, 158–162. [[CrossRef](#)]
67. Latthe, S.S.; Imai, H.; Ganesan, V.; Rao, A.V. Porous superhydrophobic silica films by sol–gel process. *Microporous Mesoporous Mater.* **2010**, *130*, 115–121. [[CrossRef](#)]
68. Lin, J.; Chen, H.; Fei, T.; Zhang, J. Highly transparent superhydrophobic organic–inorganic nanocoating from the aggregation of silica nanoparticles. *Colloids Surf.* **2013**, *421*, 51–62. [[CrossRef](#)]
69. Robles, E.; Csóka, L.; Labidi, J. Effect of reaction conditions on the surface modification of cellulose nanofibrils with aminopropyl triethoxysilane. *Coatings* **2018**, *8*, 139. [[CrossRef](#)]
70. Popescu, C.M.; Popescu, M.C.; Vasile, C. Characterization of fungal degraded lime wood by FT-IR and 2D IR correlation spectroscopy. *Microchem. J.* **2010**, *95*, 377–387. [[CrossRef](#)]
71. Han, L.; Guo, J.; Tian, X.; Jiang, X.; Yin, Y. Evaluation of PEG and Sugars Consolidated Fragile Waterlogged Archaeological Wood Using Nanoindentation and ATR-FTIR Imaging. *Int. Biodeterior. Biodegrad.* **2022**, *170*, 105390. [[CrossRef](#)]

Disclaimer/Publisher’s Note: The statements, opinions and data contained in all publications are solely those of the individual author(s) and contributor(s) and not of MDPI and/or the editor(s). MDPI and/or the editor(s) disclaim responsibility for any injury to people or property resulting from any ideas, methods, instructions or products referred to in the content.